Neurochemistry International 131 (2019) 104551

Contents lists available at ScienceDirect

Neurochemistry International

journal homepage: www.elsevier.com/locate/neuint

Noradrenaline is crucial for the substantia nigra dopaminergic cell maintenance

Sara af Bjerkén[a,b,*], Rasmus Stenmark Persson[a,b], Anna Barkander[a], Nina Karalija[c,d], Noelia Pelegrina-Hidalgo[a], Greg A. Gerhardt[e], Ana Virel[a], Ingrid Strömberg[a]

[a] Department of Integrative Medical Biology, Umeå University, Umeå, Sweden
[b] Department of Clinical Science, Neurosciences, Umeå University, Umeå, Sweden
[c] Department of Radiation Sciences, Umeå University, Umeå, Sweden
[d] Umeå Center for Functional Brain Imaging (UFBI), Umeå University, Umeå, Sweden
[e] Department of Anatomy and Neurobiology, University of Kentucky, Center for Microelectrode Technology, Lexington, KY, USA

ARTICLE INFO

Keywords:
Parkinson's disease
Noradrenaline
Dopamine
In vivo chronoamperometry
In vivo amperometry
DSP4

ABSTRACT

In Parkinson's disease, degeneration of substantia nigra dopaminergic neurons is accompanied by damage on other neuronal systems. A severe denervation is for example seen in the locus coerulean noradrenergic system. Little is known about the relation between noradrenergic and dopaminergic degeneration, and the effects of noradrenergic denervation on the function of the dopaminergic neurons of substantia nigra are not fully understood. In this study, N-(2-chloroethyl)-N-ethyl-2-bromobenzylamine (DSP4) was injected in rats, whereafter behavior, striatal KCl-evoked dopamine and glutamate releases, and immunohistochemistry were monitored at 3 days, 3 months, and 6 months. Quantification of dopamine-beta-hydroxylase-immunoreactive nerve fiber density in the cortex revealed a tendency towards nerve fiber regeneration at 6 months. To sustain a stable noradrenergic denervation throughout the experimental timeline, the animals in the 6-month time point received an additional DSP4 injection (2 months after the first injection). Behavioral examinations utilizing rotarod revealed that DSP4 reduced the time spent on the rotarod at 3 but not at 6 months. KCl-evoked dopamine release was significantly increased at 3 days and 3 months, while the concentrations were normalized at 6 months. DSP4 treatment prolonged both time for onset and reuptake of dopamine release over time. The dopamine degeneration was confirmed by unbiased stereology, demonstrating significant loss of tyrosine hydroxylase-immunoreactive neurons in the substantia nigra. Furthermore, striatal glutamate release was decreased after DSP4. In regards of neuroinflammation, reactive microglia were found over the substantia nigra after DSP4 treatment. In conclusion, long-term noradrenergic denervation reduces the number of dopaminergic neurons in the substantia nigra and affects the functionality of the nigrostriatal system. Thus, locus coeruleus is important for maintenance of nigral dopaminergic neurons.

1. Introduction

Parkinson's disease is characterized by progressive degeneration of dopaminergic neurons in the substantia nigra, leading to reduced levels of dopamine in the striatum. However, in recent years attention has also been drawn to cell death occurring in other nuclei than the nigral. For instance, an extensive loss of noradrenaline-producing neurons in the brainstem nucleus locus coeruleus has been associated with Parkinson's disease (Braak et al. 2003; Chan-Palay and Asan, 1989), and the loss of noradrenergic neurons has been reported as more pronounced than the loss of dopaminergic neurons (Zarow et al. 2003). The locus coeruleus projections target widespread areas over the brain, including the substantia nigra and ventral tegmental area (Collingridge et al. 1979; Jones and Moore, 1977), where dopaminergic neurons are located (Zarow et al. 2003). Although the noradrenergic cell loss in the locus coeruleus has been identified in Parkinson's disease, the consequence of this degeneration and the temporal relation between noradrenergic and dopaminergic cell loss remain unclear.

In 2003, Braak and co-workers proposed a Parkinson's disease staging model, suggesting alpha-synuclein propagation and Lewy body pathology to occur in a specific and predictable topographic pattern with a more peripheral onset, starting in the vagal nerve and/or the olfactory system and thereafter propagating further into the central nervous system, affecting the locus coeruleus prior to the substantia

* Corresponding author. Department of Integrative Medical Biology, Johan Bures väg 12, Umeå University, 901 87 Umeå, Sweden.
E-mail address: sara.af.bjerken@umu.se (S. af Bjerkén).

https://doi.org/10.1016/j.neuint.2019.104551
Received 25 June 2019; Received in revised form 3 September 2019; Accepted 19 September 2019
Available online 19 September 2019

Abbreviations

DSP4	N-(2-chloroethyl)-N-ethyl-2-bromobenzylamine
i.p.	Intraperitoneal
rpm	revolutions per minute
MEA	microelectrode arrays
AP	anterio-posterior
ML	medio-lateral
DV	dorso-ventral
BSA	bovine serum albumin
m-PD	1,3-phenylenediamine
PBS	phosphate buffered saline
DBH	dopamine-beta-hydroxylase
TH	tyrosine hydroxylase
Iba1	ionized calcium-binding adapter molecule 1
ir	immunoreactive
NET	noradrenaline transporter
SERT	serotonin transporter
DAT	dopamine transporter

nigra (Braak et al. 2003). This theory, known as the Braak hypothesis, has in recent years gained support from both *in vitro* and *in vivo* studies demonstrating prion-like properties of alpha-synuclein, with a cell-to-cell spread and seeding of misfolded proteins (Desplats et al. 2009; Hansen et al. 2011; Kordower et al. 2011). The hypothesis that Parkinson's disease might have a peripheral origin is supported by observations of Lewy bodies in the enteric nervous system of Parkinson's disease patients many years before development of typical clinical symptoms (Hilton et al. 2014; Shannon et al. 2012; Stokholm et al. 2016). There are, however, discrepancies in the Braak staging scheme in Parkinson's disease, which involve the proposed caudal-to-rostral evolution of the disease, and the fact that not all patients follow the outlined staging system (Parkkinen et al. 2008; Zaccai et al. 2008). There is mismatch at symptom onset between the loss of nigral dopaminergic neurons and loss of striatal dopaminergic nerve fibers, with considerably more striatal nerve fibers lost compared to nigral dopaminergic neurons, implicating a rostral-to-caudal disease spread (Tagliaferro and Burke, 2016). Nevertheless, independent of direction of α-synuclein propagation, the effects of locus coeruleus degeneration on dopaminergic neuronal function is still unclear.

Neuroinflammation is proposed as another contributing factor in Parkinson's disease. Previous studies have suggested that noradrenaline suppresses neuroinflammation (Feinstein et al. 2002; Heneka et al. 2003; Marien et al. 2004; Mavridis et al. 1991) by affecting microglial production of proinflammatory cytokines (Heneka et al. 2010). This theory is strengthened by observations demonstrating that noradrenergic hyperinnervation protects the nigrostriatal dopaminergic neurons from neurotoxins (Kilbourn et al. 1998). Notably, increased dopaminergic neuron vulnerability has been found in animals with a noradrenergic depleted locus coeruleus (Heneka et al. 2003; Marien et al. 2004; Mavridis et al. 1991), and increased dopaminergic graft survival is seen when nigral neurons are co-grafted with locus coeruleus (Berglöf and Strömberg, 2009). In view of the neuroprotective properties of noradrenaline for nigral dopaminergic neurons, it seems plausible that degeneration of noradrenergic fibers and neurons might be part of the etiology behind Parkinson's disease. Degeneration of the locus coeruleus neurons has, in fact, been suggested to precede and promote the nigral cell death in Parkinson's disease, but the dynamics of this relationship remains elusive (Del Tredici and Braak, 2013; Zarow et al. 2003).

The aim of the present work was to investigate the interaction between the noradrenergic and the dopaminergic systems. For this purpose, selective noradrenergic denervation was induced with N-(2-chloroethyl)-N-ethyl-2-bromobenzylamine (DSP4; Jonsson et al. 1981; Archer et al. 1984), and consequences from such were assessed on the striatal dopamine system, and the temporal relation between noradrenergic and dopaminergic cell loss in rats.

2. Material and methods

2.1. Animals

Female Sprague-Dawley rats weighing 150–180 g at purchase (Taconic, Ry, Denmark) were used in this study. The animals were housed under a 12:12 h light-dark cycle with *ad libitum* access to pellets and water. All experiments were approved by the local animal ethics committee.

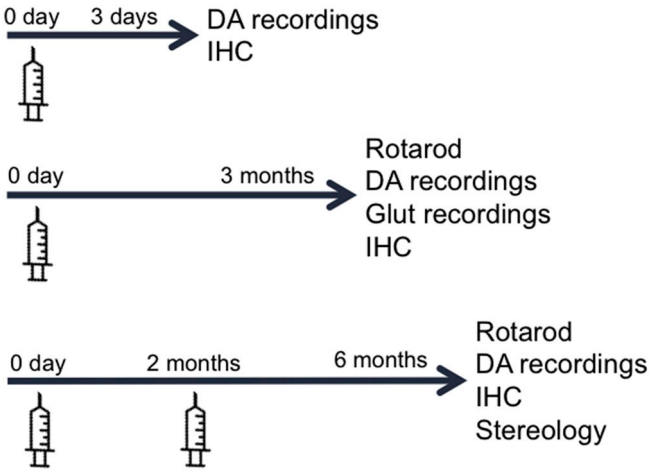

Fig. 1. Scheme illustrating the study design. The three time lines (with arrowheads) depict the experimental time points (3 days, 3 months, 6 months). Syringes illustrate treatment with intraperitoneal injections of DSP4 or saline. DA = dopamine, Glut = glutamate, IHC = immunohistochemistry.

2.2. Study design

Study design is described in Fig. 1. Rats were administered with one or two injections of either saline or DSP4 (50 mg/kg) and thereafter evaluated via behavioral assessments, electrochemical recordings, and immunohistochemistry. The dopamine recordings were performed using *in vivo* chronoamperometry at 3 days, 3 months, and 6 months. Since the chronoamperometric recordings are terminal, the functional impact on the glutamate system was analyzed in a separate set of saline/DSP4-treated animals. Striatal glutamate levels were analyzed 3 months following drug administration using *in vivo* amperometry. After electrochemical assessments, the animals were sacrificed and the brains sectioned and evaluated using immunohistochemistry and unbiased stereology. During the study, the impact on the motor coordination was analyzed in a subset of animals using rotarod performance test.

2.3. Noradrenergic denervation

Selective denervation of the locus coeruleus noradrenergic nerve terminals was performed via systemic DSP4 (50 mg/kg; Sigma-Aldrich/Merck, Darmstadt, Germany) injections. The toxin was dissolved in 0.9% NaCl and thereafter immediately injected intraperitoneally (i.p). The lesion effect was evaluated at 3 days (DSP4 x 1, $n = 10$), 3 months (DSP4 x 1, $n = 10$), and 6 months (DSP4 x 1, $n = 10$) following DSP4 administration using dopamine-beta–hydroxylase (DBH) immunohistochemistry. Saline-injected animals served as controls (3 days,

$n = 10$; 3 months, $n = 6$; 6 months, $n = 6$). Following noradrenergic nerve fiber evaluation, we decided to administer a second dose of DSP4 to animals kept in experiment longer than 3 months. That is, a booster dose was administered to the 6-month time point (DSP4 x 2, $n = 10$; saline x 2, $n = 4$), to sustain a stable noradrenergic denervation throughout the experiment. The additional dose was administered 2 months after the first administration. The different 6-month saline control groups (saline x 1 and saline x 2) did not differ in regards of DBH-immunoreactive (-ir) nerve fiber density and was therefore bundled and considered as one group ($n = 10$, $t_8 = 0.87$, $p = 0.41$) throughout the study. Two of the animals in the 3-day group were not denervated and therefore excluded from the study.

2.4. Behavioral testing

To assess the motor coordination of the animals, an accelerating rotarod (Med Associates Inc., USA) was used. The rotarod consisted of a suspended rod, accelerating from 4 to 40 revolutions per minute (rpm) during a 5-min time period. A trial started when the animal was placed on the rod and was stopped when the rat fell off the rod or after 300 s. Three consecutive trials were performed with a 15 min period of rest in between and the mean time spent on the rotarod was thereafter calculated. The rats had undergone training at three occasions prior to experiment. The mean weights for the different groups were as follows: 3 months, DSP4 x 1–249 g, saline - 266 g; 6 months, DSP4 x 2–319 g, saline - 340 g.

2.5. In vivo electrochemical recordings

In vivo electrochemistry was used to study extracellular dopamine and glutamate levels in the striatum of DSP4-lesioned and control animals. Dopamine recordings were performed in individual subjects at 3 days (DSP4 x 1, $n = 5$; saline, $n = 5$), 3 months (DSP4 x 1, $n = 5$; saline, $n = 5$), and 6 months (DSP4 x 2, $n = 7$; saline, $n = 8$). For glutamate, the recordings were performed at 3 months (DSP4 x 1, $n = 7$; saline, $n = 6$). Recordings were performed using the Fast Analytical Sensing Technology (FAST-16) system (Quanteon, Nicholasville, KY, USA; Hoffman and Gerhardt, 1998). Prior to recordings the rats were anesthetized with urethane (1.25 g/kg), tracheotomized to facilitate spontaneous breathing, and placed on a heating pad to keep adequate body temperature. The skull was fixed in a stereotaxic frame, the scalp removed, and the bone overlying the striatum bilaterally removed using a dental drill. In addition, a mm-wide hole was drilled caudally to the striatum and an Ag/AgCl reference electrode implanted. The electrodes were calibrated (procedures described below) and assembled together with a micropipette using sticky wax (130–160 μm distance between the tips for dopamine carbon fiber electrodes and 50–100 μm for glutamate microelectrode arrays; MEA). The micropipettes were filled with potassium chloride (KCl; 120 mM for dopamine recordings, 70 mM for glutamate recordings) solution and connected to a micropressure system allowing precise ejections into the brain. The ejection volumes were monitored using a scale fitted in the ocular of an operating microscope. The electrode/pipette assembly was lowered into the striatum using a microdrive.

2.5.1. In vivo chronoamperometry

Dopamine release was quantified in the striatum of DSP4-lesioned and control animals at 3 days, 3 months, and 6 months following DSP4 injection using carbon fiber electrodes and *in vivo* chronoamperometry (van Horne et al. 1992). The technique allows for second-by-second monitoring of electrochemically active compounds with high temporal and spatial resolution. In brief, single carbon fiber electrodes were coated with Nafion (Sigma-Aldrich/Merck, Darmstadt, Germany). A square-wave potential of 0–0.55 V was applied at 5 Hz causing oxidation and subsequent reduction of analytes found in close proximity to the electrode tip. The resulting currents from the oxidation/reduction reactions were integrated to an average signal per second by the FAST software. Increased extracellular analyte levels induce a rapid change in current, directly proportional to analyte concentration (Scatton et al. 1988). Increments in analyte concentration results in a peak formation, in which the highest point (with the baseline as a reference), correspond to the maximum peak amplitude (μM). Reduction/oxidation ratios were monitored to distinguish between biogenic amines, where 0.8 corresponds to dopamine, 0.2 to 5-HT, and 0.6 to noradrenaline (Strömberg et al. 1991). Electrode calibration was performed using standard solutions of ascorbic acid and dopamine, in accordance with previously described protocols (Gerhardt et al. 1984). The electrodes used in the study recorded dopamine in a linear manner ($R^2 > 0.995$), with high selectivity over ascorbic acid (200:1), and with a limit of detection < 0.05 μM when signal to noise ratio was set at 3:1. The recordings were performed at the following coordinates (in mm calculated from bregma): anterio-posterior (AP) = 0 and + 0.1, mediolateral (ML) = ± 2.6 and dorso-ventral (DV) = −3.5, −4.5, −5.5. The striatal location (starting hemisphere for each animal) for the first recordings was alternated and balanced within each group of animals. Ejections of 240 nl KCl were performed in intervals of 5 min.

2.5.2. In vivo amperometry

Recordings of striatal glutamate release and glutamate basal levels (μM) were performed in DSP4-lesioned animals and control animals at 3 months following DSP4 injection using *in vivo* amperometry and enzyme-coated ceramic-based microelectrode arrays (MEAs; Burmeister et al. 2000). A detailed description of *in vivo* amperometric recordings of glutamate has been published previously (Hascup et al. 2007), and was here followed with some minor modifications. For the experiments, electrodes (Thin-Film Technologies, Inc., Buellton, CA, USA) with four channels (333 × 15 μm) arranged in two pairs (sites separated by 30 μm for each pair) were used. Different coatings were applied to the channels, creating one pair of recording sites detecting glutamate and one pair, located 100 μm from the first pair, acting as sentinel sites. This so called self-referencing approach produces, by subtraction of interfering signals, a more specific glutamate signal (Burmeister and Gerhardt, 2001). The glutamate recording sites were coated with a solution of l-glutamate oxidase (1%), bovine serum albumin (BSA, 1%), and glutaraldehyde (0.125%). When glutamate reaches the electrode surface, it is degraded by l-glutamate oxidase into α-ketoglutarate and hydrogen peroxide (H_2O_2). H_2O_2, in contrast to glutamate, is an oxidizable compound, and detectable by the electrode (Day et al. 2006). The sentinel sites were coated with a BSA/glutaraldehyde solution, resulting in a matrix with similar properties as at the recording sites but without the ability to record glutamate. Hence, by subtracting the current recorded at the sentinel sites from the current recorded at the glutamate detecting sites, a signal specific for glutamate is produced. In addition, glutamate oxidase is considered a selective enzyme (Bohmer et al. 1989), and thus, unwanted enzymatic reactions are not a concern. After the coating procedure, electrodes were left to dry for a minimum of 72 h. An additional size-excluding coat was thereafter applied to all four channels through an electroplating procedure with 1,3-phenylenediamine (m-PD, 5 mM), to block interfering molecules such as ascorbic acid from reaching the recording sites. The electrodes were used for recordings earliest 24 h after the electroplating procedure. Calibration of the coated electrodes was performed prior to recordings to ensure selective detection of glutamate. The calibration process was undertaken at 37 °C in a beaker with 40 ml phosphate buffered saline (PBS, 0.05 M, pH = 7.4) with an Ag/AgCl electrode as reference. A constant potential of 0.7 V was applied at 2 Hz using the FAST-16 system and software and the signal was amplified 500 × (2 nA/V). Standard solutions of ascorbic acid and glutamic acid were added to the beaker to produce a final concentration of 250 μM of ascorbic acid and 60 μM of glutamic acid, where the latter was achieved by three subsequent 20 μM increments. The resulting current produced upon each addition was measured and electrodes were included when detecting

glutamate in a linear manner ($R^2 > 0.99$), with a selectivity of > 20:1 over ascorbic acid, and with a limit of detection < 2 μM, with a signal-to-noise level set at 3:1. Standard solutions of dopamine and H_2O_2 were added to the beaker (2 and 8.8 μM, respectively) at the end of the calibration, to assure impermeability of larger molecules and to test electrode sensitivity to the reporter molecule H_2O_2. Recordings were performed at the following striatal positions (in mm calculated from bregma): AP = 0 and + 0.1, ML = ± 2.6 and DV = −3.5, −4.5, in both hemispheres. At each striatal recording site, a stable baseline was acquired, and basal glutamate concentration and glutamate release was recorded. Calibrated volumes of 100 nl KCl was pressure-ejected at the recording sites at 2 min intervals to evoke glutamate release. The releases were calculated in μM above baseline. The hemisphere and striatal position for the first measurement was alternated between the subjects of each experimental group. The first KCl-evoked release was excluded at every striatal recording site in order to avoid priming effects.

2.6. Tissue processing and immunohistochemistry

Following *in vivo* electrochemical recordings, animals were transcardially perfused with calcium-free Tyrode solution followed by 4% paraformaldehyde in 0.1 M phosphate buffer. The brains were dissected out from the skull and postfixed for 24 h in 4% paraformaldehyde. Thereafter brains were thoroughly rinsed in 10% sucrose and 0.01% NaN_3 in 0.1 M phosphate buffer. Brains were frozen in CO_2 and 40 and 12 μm thin cryostat sections were then mounted and thawed onto chromealun-gelatin-coated glass slides. Sections were incubated for 48 h at 4 °C with the following primary antibodies: dopamine-beta-hydroxylase (DBH; mouse anti-DBH, 1:150; Millipore, Temecula, CA, USA), tyrosine hydroxylase (TH; rabbit anti-TH, 1:300; Millipore, Temecula, CA, USA or mouse anti-TH, 1:1500; Immunostar, Hudson, WI, USA), serotonin transporter (SERT; mouse anti-SERT, 1:100; Millipore, Temecula, CA, USA) or ionized calcium-binding adapter molecule 1 (Iba1; rabbit anti-Iba1, 1:1000; Wako Chemicals GmbH, Neuss, Germany). Sections were thereafter incubated with secondary antibodies for 4 h (40 μm) or 1 h (12 μm) at room temperature. The secondary antibodies used were Alexa Fluor®-conjugates- A594 goat anti-mouse (1:500; Molecular Probes, Leiden, The Netherlands), A488 goat anti-rabbit, (1:500; Molecular Probes, Leiden, The Netherlands). All antibodies were diluted in 0.3% Triton-X100.5% goat serum (diluted in PBS and applied for 15 min in room temperature) was used as a blocking agent prior to the secondary antibody. Sections stained with either DBH or Iba1 were also processed for TH. The sections were rinsed three times in PBS between incubations.

2.7. Unbiased stereological cell counts

Quantitative estimates of total numbers of TH-immunoreactive (-ir) neurons in the locus coeruleus and substantia nigra were determined at 6 months (DSP4 x 2/saline) using stereological cell counting. Serial sections through the locus coeruleus and substantia nigra were analyzed using the optical fractionator (West et al. 1991) and the Stereo Investigator stereological software (MBF Bioscience, Williston, VT, USA). The software was coupled to a fluorescence microscope with a computer-controlled *x-y-z* motorized stage. Cell counting was

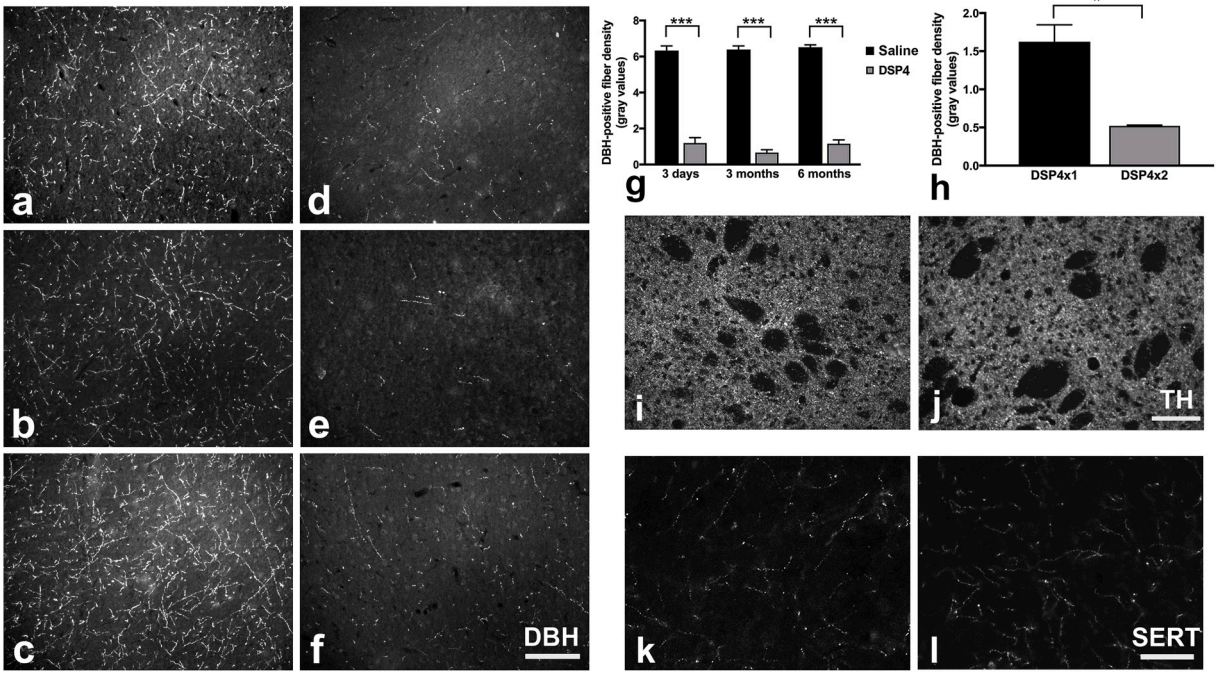

Fig. 2. DSP4-induced nerve fiber denervation. Photomicrographs of DBH-ir nerve fibers in cortex (a–f). The left panel display DBH-ir fibers in controls at 3 days (saline x 1, a), 3 months (saline x 1, b) and 6 months (saline x 1, c) following a systemic injection, whereas the right panel display the effect of the DSP4 (50 mg/kg)-lesion at 3 days (DSP4 x 1, d), 3 months (DSP4 x 1, e) and 6 months (DSP4 x 1, f), scale bar: 100 μm. Fiber density measurements (g) revealed significantly reduced DBH-ir nerve fibers already at 3 days (saline, $n = 10$; DSP4 x 1, $n = 10$) following a single systemic DSP4-administration. This effect was persistent at 3 months (saline, $n = 6$; DSP4 x 1, $n = 10$) following administration. However, at 6 months (saline, $n = 6$; DSP4 x 1, $n = 10$) a small tendency towards nerve fiber regeneration was seen (although still significantly different). To maintain DBH-ir nerve fiber denervation throughout the experiment two systemic DSP4 injections (separated by 2 months) were administered to animals kept 6 months in the experiment (h). Statistical analysis revealed significantly lower DBH-ir nerve fiber levels in the animals administered with two DSP4 injections (DSP4 x 2, $n = 10$) compared to animals administered a single injection of DSP4 (DSP4 x 1, $n = 10$). $^*p < 0.05$ $^{***}p < 0.001$.

Photomicrographs depicting striatal TH-ir nerve fiber density at 3 days (saline, i; DSP4 x 1, j; scale bar: 100 μm) and striatal SERT-ir nerve fiber density at 3 months (saline, k; DSP4 x 1, l; scale bar: 50 μm). No obvious difference was found in either TH-ir nerve fiber density or SERT-ir nerve fiber density between the treatment groups.

performed on 40 μm serial sections through the areas of interest. Since the selection of the first section in the caudal position varied from brain to brain, a random systematic design was ensured. Prior to counting, the average section thickness was measured on a number of sections from different brains. As the sections were mounted in aqueous medium, there was no significant shrinkage from the original 40 μm thickness. A guard height of 2 μm was used with a sampling brick depth of 20 μm. Pilot studies were performed to determine suitable counting frame and sampling grid dimensions prior to counting, with a counting frame size set to count around 5 neurons per frame. Outline contours were drawn at low magnification (10 ×) and the outlined region measured with a systematic random design of dissector-counting frames. The slides were coded and TH-ir cells were counted using a 60 × objective lens with a 1.4 numerical aperture.

The substantia nigra outline contours included *pars compacta* and *pars lateralis* (containing predominately TH-ir dopaminergic neurons) and excluded *pars reticulata* (containing mostly TH-ir fibers). For the substantia nigra, 7–8 sections from a 1:8 series were analyzed for each brain. Counting frame was set to, width (X) 100,5 μm, height (Y) 75,67 μm, with a depth of 20 μm. Sampling grid area was 180 × 180 μm.

The locus coeruleus outline contours were drawn to only include the A6 noradrenaline cells (Hökfeldt et al., 1984). For locus coeruleus, 5–6 sections from a 1:5 series were analyzed for each brain. Counting frame was set to, width (X) 61,55 μm, height (Y) 46,34 μm, with a depth of 20 μm. Sampling grid area was 90 × 90 μm. Systematic random sampling was implemented by the Stereoinvestigator software until the regions of interest were covered.

2.8. 8 Statistical analyses

The optical DBH- ir nerve fiber density was measured in the frontal cortex and expressed as gray values. Measurements were performed on blind-coded slides based on images captured with a CCD camera (ProgRes C14; Jenaoptik, Jena, Germany). NIH image 1.61 (software; National Institute of Health) was used to produce the gray density from binary images. Mean values for each brain were calculated from three images.

The electrochemical data collected from different striatal recording sites were statistically homogenous and therefore bundled for each group to provide a representative estimation of the dopamine and glutamate release in the striatum as a whole structure. This approach is supported by previous studies (Lundblad et al. 2009; Nevalainen et al. 2011). To describe the kinetics of KCl-evoked dopamine release, three different parameters during each time point were examined: peak amplitude (maximum concentration (μM) recorded after KCl-stimulation), T_{rise} (time until maximal concentration is reached), and T_{80} (time until the peak amplitude has decreased 80% from its maximum value). Moreover, to determine extracellular glutamate concentration, the baseline value was averaged over 30 s before first KCl ejection. This was performed by subtracting the current recorded by the sentinel channel from the signal taken up by the recording channel, hence providing assessment of the resting extracellular glutamate concentration (μM). Upon each KCl-stimulation, an increase in extracellular glutamate concentration was observed, and the maximum glutamate concentration reached (calculated from the baseline) was defined as the maximum peak amplitude and referred to as glutamate release (μM).

Statistical tests included one- or two-way analysis of variance (ANOVA). When necessary (to identify effects from dual/single factors within and between groups) the ANOVAs were followed by *Bonferroni* post hoc testing or post hoc *t*-tests. The alpha level was set at $p < 0.05$ and the results are expressed as mean value ± standard error of mean.

3. Results

3.1. DSP4-induced nerve fiber denervation

Noradrenergic denervation via DSP4-injections was evaluated by measuring the density of DBH-ir fibers in the normally densely noradrenaline innervated cortex (Fig. 2a–f). Measurements were performed at three different time points (3 days, 3 months, and 6 months) following administration of a single injection of either DSP4 or saline. A significant main effect for treatment was found, with significantly reduced DBH-ir fibers in the DSP4-treated animals compared to controls at all time points ($F_{1,\ 46} = 690.81$, $p < 0.001$, two-way ANOVA; Fig. 2g). There was a non-significant main effect of different time points ($F_{2,\ 46} = 2.31$, $p = 0.11$) and no interaction effect between treatment and time point ($F_{2,\ 46} = 1.40$, $p = 0.26$). A successful noradrenergic denervation was thus achieved using DSP4 with, at average, 18.8%, 10.3%, and 24.8% of the DBH-ir fibers remaining at 3 days, 3 months, and 6 months, respectively, when compared to the control condition. As a small tendency toward regeneration was seen at 6 months, animals kept for longer than 3 months were given two consecutive DSP4 injections to avoid regeneration and keep noradrenergic denervation throughout the experiments. Density measurements performed at 6 months and following two separate injections demonstrated desired effect, with the cortex severely devoid of DBH-ir fibers and with significantly lower nerve fiber levels compared to animals administered

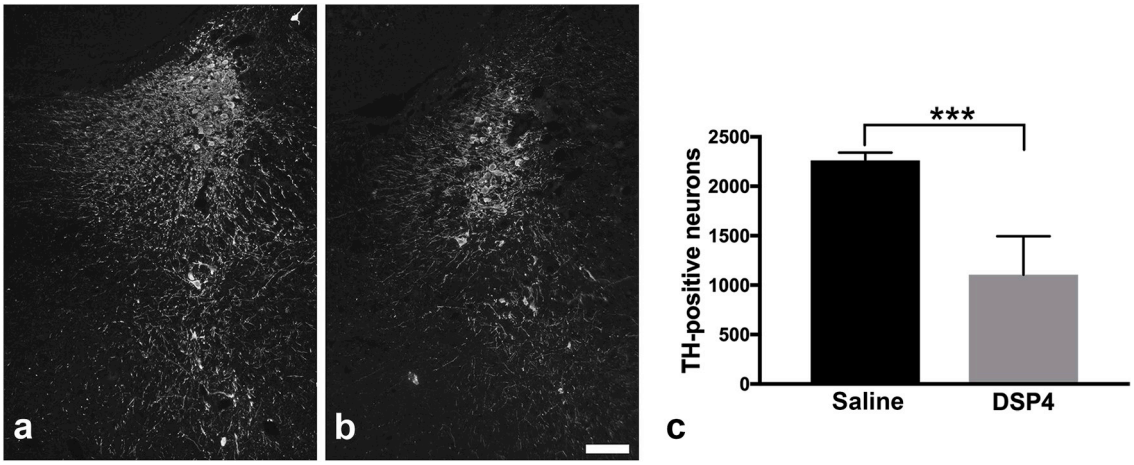

Fig. 3. Locus coeruleus TH-ir cells. Photomicrographs depicting TH-ir cells in the locus coeruleus in saline-treated (a) and DSP4-treated (b) animals at 6 months (DSP4 x 2/saline); scale bar: 100 μm. Cell quantification using unbiased stereology confirmed a significant reduction in TH-ir locus coeruleus neurons in DSP4-treated rats ($n = 9$) compared to saline controls ($n = 6$) (c). ***$p < 0.001$.

with a single DSP4 dose ($t_{12.5} = 4.70$, $p < 0.001$; Fig. 2h). Furthermore, no statistical significant difference was found between DBH-ir nerve fiber density at 3 days (DSP4 x1) and 3 months (DSP4 x 1) compared with 6 months (DSP4 x 2; $F_{2,\ 27} = 2.95$, $p = 0.07$, one-way ANOVA).

To elucidate the specificity of the denervation after DSP4 treatment, TH-ir nerve fiber density was evaluated in the striatum at 3 days after injection (DSP4 x 1/saline). The results revealed no obvious loss of TH-ir nerve fibers in the striatum, implying no acute denervation effect on the dopaminergic nerve fibers (Fig. 2i and j). In addition, evaluation of the SERT-ir nerve fiber density in the striatum, performed at 3 months (DSP4 x 1/saline), demonstrated no differences between DSP4 and saline (Fig. 2k and l).

3.2. Unbiased stereological cell counts of noradrenergic neurons

To assess the long-term effects of DSP4 administration, brains were processed for unbiased stereological cell counting, and the mean total number of TH-ir cells in the locus coeruleus was quantified at 6 months (DSP4 x 2) using the optical fractionator (West et al. 1991). Cell number quantification was performed in the locus coeruleus in the right hemisphere of each animal. The results revealed that the number of TH-ir neurons in DSP4-lesioned animals was significantly reduced in locus coeruleus compared with control animals ($t_{12.3} = 7.64$, $p < 0.001$). The saline controls had a mean total number of 2261 ± 78 TH-ir neurons compared with 1106 ± 388 for DSP4-treated animals (Fig. 3). Thus, the DSP4 treatment affected both nerve fiber density and reduced the number of neurons in the locus coeruleus.

3.3. Motoric dysfunction after DSP4 administration

To evaluate possible motor dysfunction, such as postural disturbances, a rotarod performance test was used following DSP4-induced noradrenergic denervation. At 3 months (DSP4 x 1), the DSP4-treated rats demonstrated a significant decrease in the time spent on the accelerating rotarod compared to controls ($t_{13} = 3.77$, $p < 0.01$), suggesting motoric dysfunction. The same tendency was observed at 6 months (DSP4 x 2), although not significant ($t_{13} = 2.01$, $p = 0.08$; Fig. 4).

3.4. Effects of DSP4-lesion on striatal dopamine release

To further elucidate the effects found in rotarod behavior, recordings of KCl-evoked striatal release of dopamine were performed using high-speed *in vivo* chronoamperometry (Fig. 5). The extracellular dopamine levels after local KCl-stimulation were quantified in saline- and DSP4-treated animals at different time points; 3 days (DSP4 x 1/saline), 3 months (DSP4 x 1/saline), and 6 months (DSP4 x 2/saline). The reduction/oxidation ratio for the signals was approximately 0.8, suggesting that it was dopamine that gave the signal. Since the main purpose with DSP4-treatment was to produce a stable noradrenergic lesion, and no statistical significant difference was found between DBH-ir nerve fiber density at 3 days (DSP4 x 1) and 3 months (DSP4 x 1) compared with 6 months (DSP4 x 2), the three time points were all handled within the same statistical model. A two-way ANOVA was conducted to examine the effect of treatment (DSP4 or saline) on KCl-evoked striatal dopamine release over time. DSP4-treatment resulted in significantly increased peak amplitudes of striatal dopamine when compared with saline-treatment, with significant main effects of treatment ($F_{1,\ 262} = 34.07$, $p < 0.001$) and time after the DSP4 injection ($F_{2,\ 262} = 6.69$, $p = 0.001$; Fig. 5b). No interaction effect was found between the factors ($F_{2,\ 262} = 2.30$, $p = 0.10$). To explore the data further, the main analysis was followed by three additional post hoc *t*-tests with *Bonferroni* correction (testing the hypothesis at $\alpha = 0.05/3$, i.e. considered as significant if $p < 0.0167$) between DSP4 and saline within each time point. Significantly higher peak amplitudes of KCl-evoked dopamine release were found in the DSP4-treated animals compared with controls at 3 days (DSP4 x 1 6.92 ± 0.40 μM, saline 4.45 ± 0.39 μM; $t_{85} = -4.42$, $p < 0.001$) and 3 months (DSP4 x 1 8.06 ± 0.42 μM, saline 5.34 ± 0.43 μM; $t_{90} = -4.49$, $p < 0.001$). The same tendency was observed at 6 months, although not statistically significant.

3.5. Effects of DSP4-lesion on dopamine onset and clearance

Two-way ANOVA demonstrated no significant effect of treatment on T_{rise} (time until maximal peak concentration; $F_{1,\ 259} = 1.08$, $p = 0.30$), however, T_{rise} was significantly prolonged over time ($F_{2,\ 259} = 7.02$, $p < 0.001$). The trending interaction effect was non-significant ($F_{2,\ 259} = 2.39$, $p = 0.093$). To explore the effect on time since injection, the two-way analysis was followed up by one-way ANOVAs, conducted separately for each treatment group (DSP4/saline). Whereas no significant difference in T_{rise} was found for the control group ($F_{2,\ 149} = 1.07$, $p = 0.37$), such was found within the DSP4-treated group ($F_{2,\ 110} = 5.52$, $p < 0.01$) with a significant difference between 3 days and 6 months ($p < 0.01$; Fig. 5c).

Furthermore, for T_{80}, the time measured from maximal amplitude until the concentration had reached 80% of maximal concentration, a significant main effect for time after injection was seen ($F_{2,\ 259} = 3.04$, $p < 0.05$) but no significant main effect of treatment ($F_{1,\ 259} = 0.36$, $p = 0.55$). Also, an interaction effect between the factors was found ($F_{2,\ 259} = 3.80$, $p < 0.05$).

To follow up and explore the effect on time after injection and the significant interaction effect, the two-way analysis was followed up by one-way ANOVAs, conducted separately for each treatment (DSP4/saline) as well as separate *t*-tests for each time point. For treatment, an increase in T_{80} was found in the DSP4-treated group ($F_{2,\ 110} = 4.20$, $p < 0.05$) with a significant difference between 3 days and 3 months ($p < 0.05$) and 3 days and 6 months ($p < 0.05$). No significant difference in T_{80} was found in the control group ($F_{2,\ 149} = 2.80$, $p = 0.064$). For time points, the main analysis was followed by three additional post hoc *t*-tests with *Bonferroni* correction (testing the hypothesis at $\alpha = 0.05/3$, i.e. considered as significant if $p < 0.0167$) between DSP4 and saline within each time point. These tests declared a significant difference at 3 days, with significantly reduced T_{80} in the DSP4 animals compared to saline ($t_{85} = 3.29$, $p < 0.001$; Fig. 5d).

3.6. DSP4-lesion effects on striatal glutamate release

To further study effects of the noradrenergic denervation on transmitter releases, striatal KCl-stimulated glutamate release was recorded using *in vivo* amperometry and enzyme-coated microelectrode arrays. Three months following a single dose of DSP4, i.e. the time point when significantly increased striatal dopamine release was seen, significant different levels of KCl-evoked glutamate release was found in the DSP4-treated animals with a mean release peak amplitude above baseline of

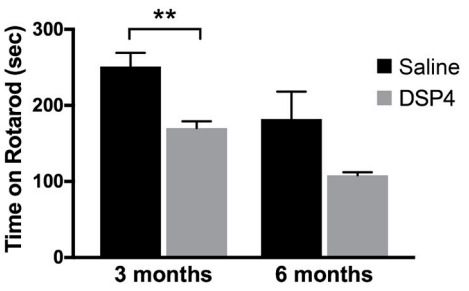

Fig. 4. Rotarod performance test. At 3 months, DSP4-treated animals managed to stay significantly shorter time periods on the rotarod compared to controls (saline, $n = 8$; DSP4 x 1, $n = 7$). The same trend, however not significant, was seen at 6 months (saline, $n = 8$; DSP4 x 2, $n = 7$). $^{**}p < 0.01$.

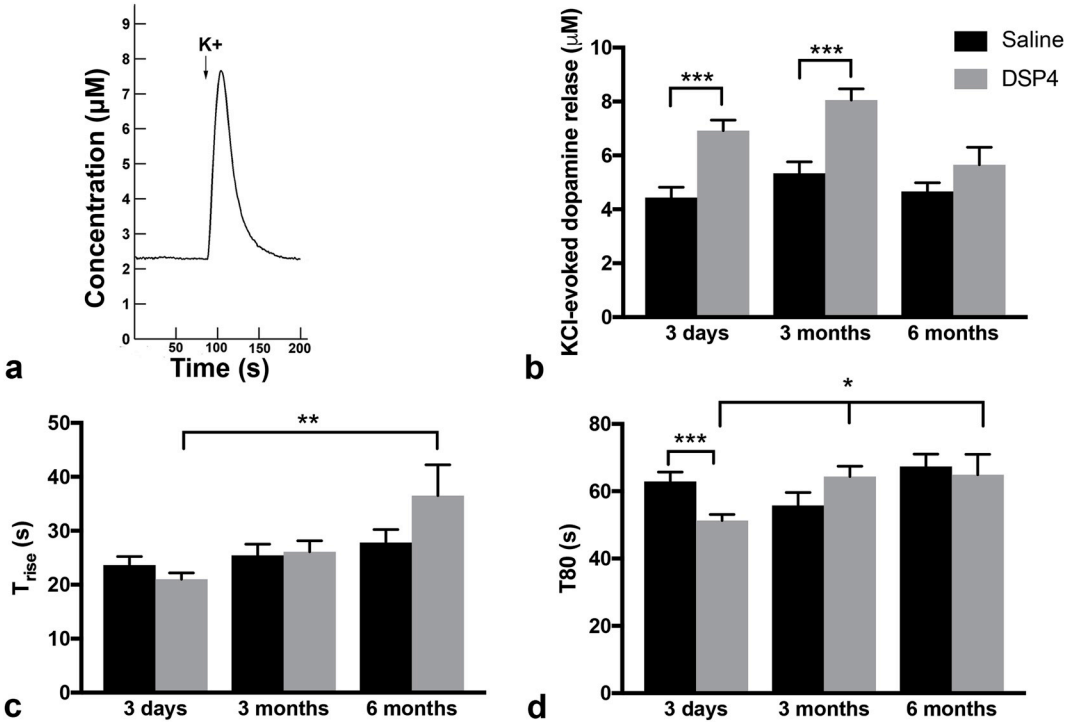

Fig. 5. Dopamine recordings. *In vivo* chronoamperometric striatal recordings of KCl-evoked dopamine release in DSP4-treated and saline-treated control animals. Signal from a single KCl-evoked (arrow) dopamine release (a). DSP4 treatment significantly increased the extracellular dopamine release (measured as peak amplitude) at 3 days, and 3 months compared with saline treatment. No significant differences in dopamine release were found at 6 months (b). An increase in T_{rise}, i.e. time in seconds needed to reach the peak amplitude (maximal concentration), was found over time within the DSP4-treated animals with significantly increased T_{rise} at 6 months compared to 3 months (c). T_{80}, measured as the time from peak amplitude until the concentration had decreased to 80% of maximal concentration, was increased within the DSP4-treated animals with significant differences between 3 days and 3 months, and between 3 days and 6 months (d). At 3 days, T_{80} was significantly reduced in the DSP4-treated animals compared with saline (measurements - saline: 3 days, $n = 48$; 3 months, $n = 48$; 6 months, $n = 56$. DSP4: 3 days, $n = 39$; 3 months, $n = 44$; 6 months, $n = 44$). $^{*}p < 0.05$, $^{**}p < 0.01$, $^{***}p < 0.001$.

approximately 4 μM compared to approximately 11 μM in intact saline-treated control animals ($t_{126.78} = 9.03$, $p < 0.001$). No difference in baseline extracellular glutamate levels was found between the animal groups, with concentrations around 4 μM in both DSP4 - and saline-treated animals ($t_{26} = 1.41$, $p = 0.16$; Fig. 6). Thus, striatal dopamine release was increased, while striatal glutamate release was reduced after DSP4 treatment.

3.7. Total TH-ir neuron number in the substantia nigra

To corroborate the results of impaired rotarod behavior and enhanced striatal dopamine release in the DSP4 animals, the number of TH-ir neurons in the substantia nigra was evaluated at 3 and 6 months. No visible loss of TH-ir neurons was found at 3 months (supplementary material; Figure S1). However, at 6 months, a difference was evident and confirmed by unbiased stereology demonstrating a significantly reduced mean total number of TH-ir neurons in the substantia nigra of DSP4-lesioned animals compared with controls ($t_{13} = 2.33$, $p < 0.05$). The DSP4-treated group (DSP4 x 2) had a mean total number of 6957 ± 347 TH-ir neurons compared with a mean total number of 8397 ± 551 for saline controls (Fig. 7).

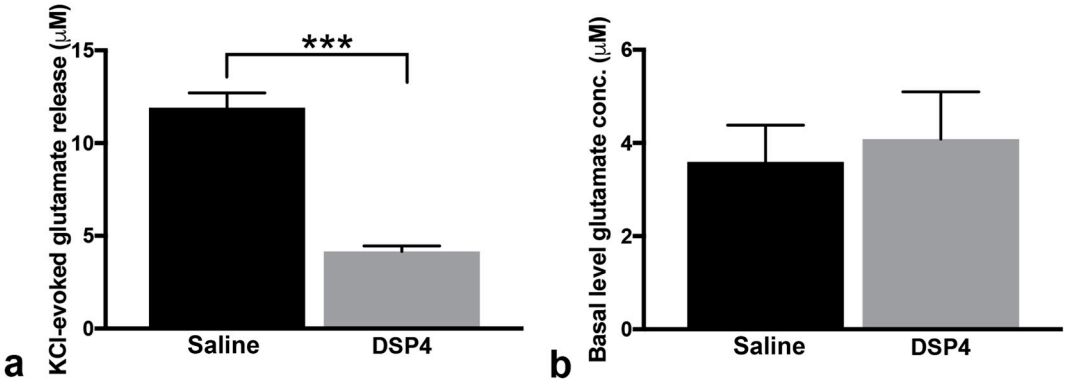

Fig. 6. Glutamate recordings. *In vivo* amperometric striatal recordings of KCl-evoked glutamate release in DSP4-treated and saline-treated control animals. Quantification of striatal glutamate at 3 months (DSP4 x 1/saline) demonstrated significantly reduced levels of glutamate in DSP4-treated animals (measurements, $n = 136$) compared to saline-treated controls (measurements, $n = 99$) (a). The concentrations are calculated above baseline. The basal extracellular glutamate concentrations, estimated by averaging the baseline, did not differ significantly between the groups (b). $^{***}p < 0.001$.

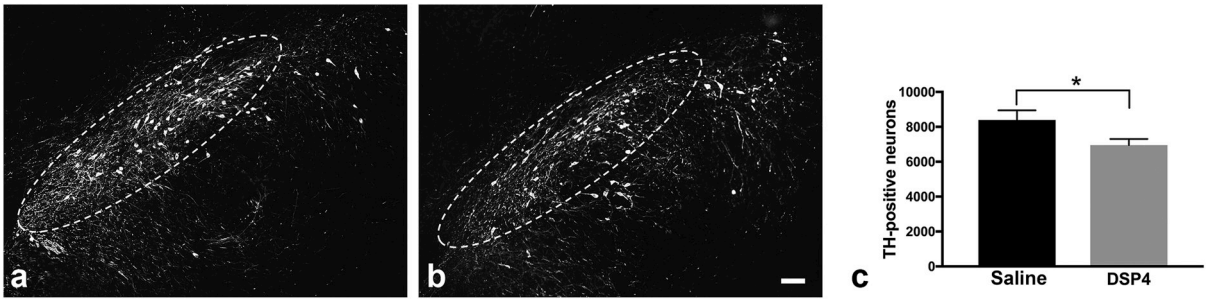

Fig. 7. Substantia nigra TH-ir cells at 6 months. Photomicrographs depicting TH-ir cells in the substantia nigra *pars compacta* (encircled) in saline-treated (a) and DSP4-treated (b) animals at 6 months (DSP4 x 2/saline); scale bar: 100 μm. Stereological cell counts of TH-ir cells in DSP4-treated rats ($n = 9$) demonstrate a significant reduction in TH-ir nigral neurons compared to saline controls ($n = 6$) (c). $^*p < 0.05$.

3.8. Iba1-ir microglia in the substantia nigra

The immunological response at 6 months following DSP4 treatment was investigated in the substantia nigra utilizing Iba1 immunohistochemistry. An evident difference in Iba1-ir morphology was found between the groups, with typical resting state Iba1-ir microglia in the control animals compared to the Iba1-ir microglia found in the DSP4 animals demonstrating typical signs of reactivity, such as a large rounded soma and short processes (Fig. 8).

4. Discussion

This study demonstrated that DSP4 significantly reduced the noradrenergic nerve fiber density in the cortex, a denervation effect seen to a similar extent from 3 days to 6 months, when administering a booster dose of DSP4 to the animals with longest survival time. Loss of DBH-ir nerve fibers was confirmed, together with an approximately 50% loss of noradrenergic neurons in the locus coeruleus. Also, DSP4 treatment impaired rotarod behavior at 3 but not at 6 months. Alterations in neurotransmission were found, with increased striatal KCl-evoked dopamine release at 3 days and 3 months after DSP4 treatment and significantly reduced striatal glutamate release at 3 months. Furthermore, DSP4 treatment prolonged both T_{rise} and T_{80} for dopamine over time when comparing within the DSP4-treated group, while the acute effect of DSP4 reduced T_{80} for dopamine. The DSP4 lesions significantly reduced the number of dopaminergic neurons in the substantia nigra at 6 months, and shifted the microglia over the same area into a morphologically reactive state. Altogether, these data indicate that a noradrenergic lesion have profound effects on the dopamine system.

DSP4 is, besides to denervate the noradrenergic system, commonly used to inhibit the noradrenaline transporter (NET). A recent *in vitro* study has, however, found that it also affects the serotonin- and dopamine transporters (SERT and DAT; Wenge and Bonisch, 2009). Though, in contrast to the strong and irreversible inhibition of NET, the inhibition of DAT and SERT was 5 and 40 times lower, respectively, and included a reversible component. This low-grade effect on the dopaminergic and serotonergic systems may therefore not be of great importance in studies using DSP4. The noradrenergic selectivity of DSP4 thus suggests that the effects found on the dopaminergic neurons in the present study are exerted via the noradrenergic system. The noradrenergic nerve fibers have previously been reported to be degenerated approximately 10 days after a DSP4 injection (Fritschy and Grzanna, 1992). While several short-term studies involving DSP4-lesioned animals have failed to demonstrate loss of locus coeruleus neurons (Szot et al. 2010; Zhang et al. 1995), we have in this study found long-term effects with loss of noradrenergic neurons at 6 months after lesion, a finding also documented by others (Fritschy and Grzanna, 1992). Even though the loss of the locus coeruleus neurons was significant at long-term time points, sprouting may occur after a single dose of DSP4 (Fritschy and Grzanna, 1992), an effect seen in the current study. Therefore, two consecutive doses of DSP4 were given for the 6 months time point, which was demonstrated to be efficient.

KCl-evoked dopamine release was increased at the earlier time points (3 days and 3 months) after the noradrenergic lesion, while at 6 months, released dopamine reached normal levels. These results are supported by another study, with initially higher levels of dopamine that normalized at longer time points (Pycock et al. 1975), while other studies demonstrate decreased striatal dopamine release and reduced metabolites after noradrenergic nerve fiber depletion as well as in DBH knock-out mice (Harro et al. 2003; Lategan et al. 1990, 1992; Schank et al. 2006; Rommelfanger and Weinshenker, 2007). Locus coeruleus neurons innervate the substantia nigra and a single-pulse stimulation of the locus coeruleus neurons evokes a dual effect, i.e. excitation followed by inhibition of the nigral neurons (Grenhoff et al. 1993). However, a

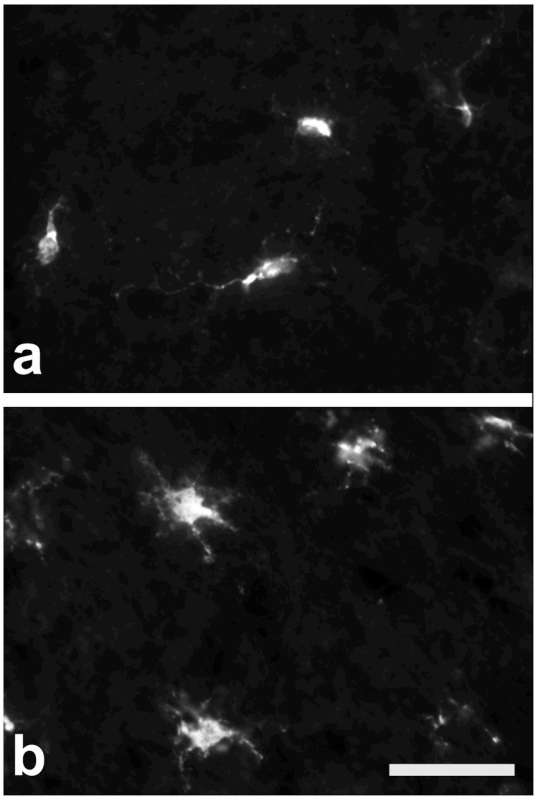

Fig. 8. Iba1-ir microglia. Photomicrographs depicting Iba1-ir microglia over the substantia nigra at 6 months. A morphological difference was found in that the microglia in saline control animals (a) appeared to be in a resting state (i.e. smaller elongated soma with thin processes) whereas the Iba1-ir microglia in DSP4 animals (DSP4 x 2; b) displayed a reactive morphology (i.e. larger amoeboid/rounded somas with short processes). Scale bar: 25 μm.

burst-like stimulation from locus coeruleus results in a long-lasting inhibition of the nigral neurons, similar to the effect reported in the axis of locus coeruleus/ventral tegmental area/nucleus accumbens (Kielbinski et al. 2019). As a consequence, a denervation of the locus coeruleus may abolish the inhibition and lead to enhanced dopamine release. Thus, locus coeruleus may exert different effects on the substantia nigra neurons depending on the firing pattern. The reduced levels of striatal glutamate release found after a DSP4 lesion may, at least partly, support the finding of increased dopamine concentrations, since dopamine inhibit striatal glutamate activity via dopamine D2 receptors located on the glutamatergic nerve terminals (Bamford et al. 2004a, 2004b).

At the earlier time points, the time to reach the maximal dopamine concentration, T_{rise}, was not changed although the final concentration was significantly higher. Seen over time, however, T_{rise} was prolonged, i.e. despite that the dopamine release was normalized at 6 months, the time needed to reach maximal dopamine concentration was longer. Further, T_{80} was significantly shorter, i.e. the clearance of extracellular dopamine occurred faster at the 3-day time point after the noradrenergic denervation, while at 6 months the dopamine reuptake occurred slower when compared within the DSP4-treated group. Thus, the long-term effect of noradrenergic denervation demonstrated that dopamine was released in normal concentrations, but by a more slowly acting dopamine system when regarding that T_{rise} was prolonged. It is known that serotonergic nerve fibers may uptake and participate in the clearance of extracellular dopamine and thereby also release of dopamine (Kannari et al. 2006), and since KCl stimulates release also from serotonergic nerve fibers this may then potentially affect the concentration of released dopamine as well as the clearance. Thus, it is possible that the increased dopamine release seen is produced by serotonergic nerve fibers. The striatal SERT-ir nerve fiber density did, however, not appear to be altered by the DSP4 treatment, suggesting a comparable magnitude of serotonergic nerve fiber involvement independent of treatment. Similar interference from reminiscent noradrenergic nerve fibers is not possible, since the striatum is missing noradrenergic innervation. However, noradrenergic nerve fibers may affect clearance of dopamine in the prefrontal cortex (Fuxe, 1965; Mazei et al. 2002; Swanson and Hartman, 1975). Furthermore, the motor behavior was impaired after the DSP4 lesion when the released dopamine levels were enhanced. The impaired behavior is supported by other investigators, who found that a noradrenergic denervation aggravates behavioral deficits in Parkinson's disease animal models (Srinivasan and Schmidt, 2003; Rommelfanger et al. 2007; Shin et al. 2014). Also, since the locus coeruleus sends projections to the ventral horn of the spinal cord (Nygren and Olson, 1977; Westlund et al. 1983) and to the cerebellum (Olson and Fuxe, 1971; Ungerstedt, 1971), it is reasonable to assume that reduced noradrenergic innervation could cause balance impairment. Indeed, depletion of noradrenaline from the cerebellum has been found to result in impaired motor performance (Watson and McElligott, 1984). Regarding the discrepancy in time spent on the rotarod between the saline controls at 3 and 6 months, it is likely explained by the weight differences.

It has been documented that loss of noradrenergic input to the substantia nigra increases the vulnerability of the dopaminergic neurons (Marien et al. 2004; Mavridis et al. 1991; Srinivasan and Schmidt, 2003; Shin et al. 2014; Rommelfanger et al. 2007; Yao et al. 2015; Farrand et al. 2017). However, here we demonstrate a direct effect of a long-term sustained noradrenergic locus coerulean lesion on the nigral dopaminergic neurons, resulting in dopaminergic cell loss. A plausible underlying mechanism might be found in the suppressive properties of noradrenaline when it comes to neuroinflammation (Heneka et al. 2003). An idea supported by our finding of altered microglia morphology over substantia nigra following DSP4 treatment, with Iba1-ir microglia exhibiting a reactive morphology. Furthermore, this microglia reaction can be counteracted if the vagus nerve is stimulated, suggesting that the microglial reactivity is mediated via loss of noradrenaline (Farrand et al. 2017). However, there is still a possibility that the reactive microglia, as well as the loss of dopaminergic neurons, might be a direct consequence of the neurotoxin. This means, DSP4 may be uptaken by the dopaminergic neurons through DAT, and thereby inhibit dopamine uptake (Wenge and Bonisch, 2009). We would then have expected a prolonged and not shortened dopamine clearance time, as found at 3 days. Moreover, it is known that the acute action of DSP4 on DAT is reversed at longer time points (Wenge and Bonisch, 2009). Thus, the loss of dopaminergic neurons seen at 6 months in the current study is most likely caused by the noradrenergic denervation, supporting the Braak theory, i.e. that a noradrenergic cell death in the locus coeruleus impacts the dopaminergic nigral neurons. There is no evidence that DSP4 toxicity involves alpha-synuclein oligomerization. However, DSP4 treatment has been found to affect alpha-synuclein, but then in combination with a dopaminergic neurotoxin (Farrand et al. 2017).

Taken together, this study clearly demonstrates the importance of an intact locus coeruleus for maintenance of the nigral dopaminergic neurons and motor function. As such, noradrenergic maintenance may play an important part in the etiology of Parkinson's disease.

Declarations of interest

None.

Acknowledgements

This study was supported by the Swedish Parkinson Foundation, the Swedish Research Council grant number #9917, The County Council of Västerbotten, The Swedish Society of Medicine, The Lars Hierta Memorial Foundation, Åhlén Foundation (Åhlén-stiftelsen), Umeå University, and the Research Foundation for Clinical Neuroscience at Umeå University Hospital. The authors have no conflicts of interests to declare.

Appendix ASupplementary data

Supplementary data to this article can be found online at https://doi.org/10.1016/j.neuint.2019.104551.

References

Archer, T., Jonsson, G., Ross, S.B., 1984. A parametric study of the effects of the noradrenaline neurotoxin DSP4 on avoidance acquisition and noradrenaline neurones in the CNS of the rat. Br. J. Pharmacol. 82, 249–257.
Bamford, N.S., Robinson, S., Palmiter, R.D., Joyce, J.A., Moore, C., Meshul, C.K., 2004a. Dopamine modulates release from corticostriatal terminals. J. Neurosci. : Off. J. Soc. Neurosci. 24, 9541–9552.
Bamford, N.S., Zhang, H., Schmitz, Y., et al., 2004b. Heterosynaptic dopamine neurotransmission selects sets of corticostriatal terminals. Neuron 42, 653–663.
Berglöf, E., Strömberg, I., 2009. Locus coeruleus promotes survival of dopamine neurons in ventral mesencephalon. An in oculo grafting study. Exp. Neurol. 216, 158–165.
Bohmer, A., Muller, A., Passarge, M., Liebs, P., Honeck, H., Muller, H.G., 1989. A novel L-glutamate oxidase from Streptomyces endus. Purification and properties. Eur. J. Biochem. 182, 327–332.
Braak, H., Del Tredici, K., Rub, U., de Vos, R.A., Jansen Steur, E.N., Braak, E., 2003. Staging of brain pathology related to sporadic Parkinson's disease. Neurobiol. Aging 24, 197–211.
Burmeister, J.J., Gerhardt, G.A., 2001. Self-referencing ceramic-based multisite microelectrodes for the detection and elimination of interferences from the measurement of L-glutamate and other analytes. Anal. Chem. 73, 1037–1042.
Burmeister, J.J., Moxon, K., Gerhardt, G.A., 2000. Ceramic-based multisite microelectrodes for electrochemical recordings. Anal. Chem. 72, 187–192.
Chan-Palay, V., Asan, E., 1989. Alterations in catecholamine neurons of the locus coeruleus in senile dementia of the Alzheimer type and in Parkinson's disease with and without dementia and depression. J. Comp. Neurol. 287, 373–392.
Collingridge, G.L., James, T.A., MacLeod, N.K., 1979. Neurochemical and electrophysiological evidence for a projection from the locus coeruleus to the substantia nigra [proceedings]. J. Physiol. 290, 44.
Day, B.K., Pomerleau, F., Burmeister, J.J., Huettl, P., Gerhardt, G.A., 2006. Microelectrode array studies of basal and potassium-evoked release of L-glutamate in the anesthetized rat brain. J. Neurochem. 96, 1626–1635.
Del Tredici, K., Braak, H., 2013. Dysfunction of the locus coeruleus-norepinephrine

system and related circuitry in Parkinson's disease-related dementia. J. Neurol. Neurosurg. Psychiatry 84, 774–783.
Desplats, P., Lee, H.J., Bae, E.J., Patrick, C., Rockenstein, E., Crews, L., Spencer, B., Masliah, E., Lee, S.J., 2009. Inclusion formation and neuronal cell death through neuron-to-neuron transmission of alpha-synuclein. Proc. Natl. Acad. Sci. U.S.A. 106, 13010–13015.
Farrand, A.Q., Helke, K.L., Gregory, R.A., Gooz, M., Hinson, V.K., Boger, H.A., 2017. Vagus nerve stimulation improves locomotion and neuronal populations in a model of Parkinson's disease. Brain Stimul. 10, 1045–1054.
Feinstein, D.L., Heneka, M.T., Gavrilyuk, V., Dello Russo, C., Weinberg, G., Galea, E., 2002. Noradrenergic regulation of inflammatory gene expression in brain. Neurochem. Int. 41, 357–365.
Fritschy, J.M., Grzanna, R., 1992. Restoration of ascending noradrenergic projections by residual locus coeruleus neurons: compensatory response to neurotoxin-induced cell death in the adult rat brain. J. Comp. Neurol. 321, 421–441.
Fuxe, K., 1965. Evidence for the existence of monoamine neurons in the central nervous system. Iv. Distribution of monoamine nerve terminals in the central nervous system. Acta Physiol. Scand. Suppl. (Suppl. 247), 237+.
Gerhardt, G.A., Oke, A.F., Nagy, G., Moghaddam, B., Adams, R.N., 1984. Nafion-coated electrodes with high selectivity for CNS electrochemistry. Brain Res. 290, 390–395.
Grenhoff, J., Nisell, M., Ferre, S., Aston-Jones, G., Svensson, T.H., 1993. Noradrenergic modulation of midbrain dopamine cell firing elicited by stimulation of the locus coeruleus in the rat. J. Neural Transm. Gen. Sect. 93, 11–25.
Hansen, C., Angot, E., Bergstrom, A.L., et al., 2011. alpha-Synuclein propagates from mouse brain to grafted dopaminergic neurons and seeds aggregation in cultured human cells. J. Clin. Investig. 121, 715–725.
Harro, J., Terasmaa, A., Eller, M., Rinken, A., 2003. Effect of denervation of the locus coeruleus projections by DSP-4 treatment on [3H]-raclopride binding to dopamine D (2) receptors and D(2) receptor-G protein interaction in the rat striatum. Brain Res. 976, 209–216.
Hascup, K.N., Rutherford, E.C., Quintero, J.E., Day, B.K., Nickell, J.R., Pomerleau, F., Huettl, P., Burmeister, J.J., Gerhardt, G.A., 2007. Second-by-Second measures of L-glutamate and other neurotransmitters using enzyme-based microelectrode arrays. In: Michael, A.C., Borland, L.M. (Eds.), Electrochemical Methods for Neuroscience, Boca Raton (FL).
Heneka, M., Gavriluyk, V., Landreth, G., O'Banion, M., Weinberg, G., Feinstein, D., 2003. Noradrenergic depletion increases inflammatory responses in brain: effects on kappaB and HSP70 expression. J. Neurochem. 85, 387–398.
Heneka, M.T., Nadrigny, F., Regen, T., et al., 2010. Locus ceruleus controls Alzheimer's disease pathology by modulating microglial functions through norepinephrine. Proc. Natl. Acad. Sci. U.S.A. 107, 6058–6063.
Hilton, D., Stephens, M., Kirk, L., Edwards, P., Potter, R., Zajicek, J., Broughton, E., Hagan, H., Carroll, C., 2014. Accumulation of alpha-synuclein in the bowel of patients in the pre-clinical phase of Parkinson's disease. Acta Neuropathol. 127, 235–241.
Hoffman, A.F., Gerhardt, G.A., 1998. In vivo electrochemical studies of dopamine clearance in the rat substantia nigra: effects of locally applied uptake inhibitors and unilateral 6-hydroxydopamine lesions. J. Neurochem. 70, 179–189.
Hökfeldt, T., Mårtensson, R., Björklund, A., Kleinau, S., Goldstein, M., 1984. Distributional maps of tyrosine-hydroxylase-immunoreactive neurons in the rat brain. In: Handbook of Chemical Neuroanatomy, vol. 2 Elsevier Science Publishers B.V.
Jones, B.E., Moore, R.Y., 1977. Ascending projections of the locus coeruleus in the rat. II. Autoradiographic study. Brain Res. 127, 25–53.
Jonsson, G., Hallman, H., Ponzio, F., Ross, S., 1981. DSP4 (N-(2-chloroethyl)-N-ethyl-2-bromobenzylamine)–a useful denervation tool for central and peripheral noradrenaline neurons. Eur. J. Pharmacol. 72, 173–188.
Kannari, K., Shen, H., Arai, A., Tomiyama, M., Baba, M., 2006. Reuptake of L-DOPA-derived extracellular dopamine in the striatum with dopaminergic denervation via serotonin transporters. Neurosci. Lett. 402, 62–65.
Kielbinski, M., Bernacka, J., Solecki, W.B., 2019. Differential regulation of phasic dopamine release in the forebrain by the VTA noradrenergic receptor signaling. J. Neurochem. 149, 747–759.
Kilbourn, M., Sherman, P., Abbott, L., 1998. Reduced MPTP neurotoxicity in striatum of the mutant mouse *tottering*. Synapse 30, 205–210.
Kordower, J.H., Dodiya, H.B., Kordower, A.M., Terpstra, B., Paumier, K., Madhavan, L., Sortwell, C., Steece-Collier, K., Collier, T.J., 2011. Transfer of host-derived alpha synuclein to grafted dopaminergic neurons in rat. Neurobiol. Dis. 43, 552–557.
Lategan, A.J., Marien, M.R., Colpaert, F.C., 1990. Effects of locus coeruleus lesions on the release of endogenous dopamine in the rat nucleus accumbens and caudate nucleus as determined by intracerebral microdialysis. Brain Res. 523, 134–138.
Lategan, A.J., Marien, M.R., Colpaert, F.C., 1992. Suppression of nigrostriatal and mesolimbic dopamine release in vivo following noradrenaline depletion by DSP-4: a microdialysis study. Life Sci. 50, 995–999.
Lundblad, M., af Bjerkén, S., Cenci, M.A., Pomerleau, F., Gerhardt, G.A., Strömberg, I., 2009. Chronic intermittent L-DOPA treatment induces changes in dopamine release. J. Neurochem. 108, 998–1008.
Marien, M.R., Colpaert, F.C., Rosenquist, A.C., 2004. Noradrenergic mechanisms in neurodegenerative diseases: a theory. Brain Res. Rev. 45, 38–78.
Mavridis, M., Degryse, A.-D., Lategan, A., Marien, M., Colpaert, F., 1991. Effects of loculs coeruleus lesion on parkinsonian signs, striatal dopamine and substantia nigra cell loss after 1-methyl-4-phenyl-1,2,3,6-tetrahydropyridine in monkeys: a possibel role for the locus coeruleus in the progression of Parkinson's disease. Neurosci. 41, 507–523.
Mazei, M.S., Pluto, C.P., Kirkbride, B., Pehek, E.A., 2002. Effects of catecholamine uptake blockers in the caudate-putamen and subregions of the medial prefrontal cortex of the rat. Brain Res. 936, 58–67.
Nevalainen, N., Af Bjerkén, S., Lundblad, M., Gerhardt, G.A., Strömberg, I., 2011. Dopamine release from serotonergic nerve fibers is reduced in L-DOPA-induced dyskinesia. J. Neurochem. 118, 12–23.
Nygren, L.G., Olson, L., 1977. A new major projection from locus coeruleus: the main source of noradrenergic nerve terminals in the ventral and dorsal columns of the spinal cord. Brain Res. 132, 85–93.
Olson, L., Fuxe, K., 1971. On the projections from the locus coeruleus noradrealine neurons: the cerebellar innervation. Brain Res. 28, 165–171.
Parkkinen, L., Pirttila, T., Alafuzoff, I., 2008. Applicability of current staging/categorization of alpha-synuclein pathology and their clinical relevance. Acta Neuropathol. 115, 399–407.
Pycock, C.J., Donaldson, I.M., Marsden, C.D., 1975. Circling behaviour produced by unilateral lesions in the region of the locus coeruleus in rats. Brain Res. 97, 317–329.
Rommelfanger, K.S., Edwards, G.L., Freeman, K.G., Liles, L.C., Miller, G.W., Weinshenker, D., 2007. Norepinephrine loss produces more profound motor deficits than MPTP treatment in mice. Proc. Natl. Acad. Sci. U.S.A. 104, 13804–13809.
Rommelfanger, K.S., Weinshenker, D., 2007. Norepinephrine: the redheaded stepchild of Parkinson's disease. Biochem. Pharmacol. 74, 177–190.
Scatton, B., D'Angio, M., Driscoll, P., Serrano, A., 1988. An in vivo voltammetric study of the response of mesocortical and mesoaccumbens dopaminergic neurons to environmental stimuli in strains of rats with differing levels of emotionality. Ann. N. Y. Acad. Sci. 537, 124–137.
Schank, J.R., Ventura, R., Puglisi-Allegra, S., Alcaro, A., Cole, C.D., Liles, L.C., Seeman, P., Weinshenker, D., 2006. Dopamine beta-hydroxylase knockout mice have alterations in dopamine signaling and are hypersensitive to cocaine. Neuropsychopharmacology : official publication of the American College of Neuropsychopharmacology 31, 2221–2230.
Shannon, K.M., Keshavarzian, A., Dodiya, H.B., Jakate, S., Kordower, J.H., 2012. Is alpha-synuclein in the colon a biomarker for premotor Parkinson's disease? Evidence from 3 cases. Mov. Disord. 27, 716–719.
Shin, E., Rogers, J.T., Devoto, P., Björklund, A., Carta, M., 2014. Noradrenaline neuron degeneration contributes to motor impairments and development of L-DOPA-induced dyskinesia in a rat model of Parkinson's disease. Exp. Neurol. 257, 25–38.
Srinivasan, J., Schmidt, W.J., 2003. Potentiation of parkinsonian symptoms by depletion of locus coeruleus noradrenaline in 6-hydroxydopamine-induced partial degeneration of substantia nigra in rats. Eur. J. Neurosci. 17, 2586–2592.
Stokholm, M.G., Danielsen, E.H., Hamilton-Dutoit, S.J., Borghammer, P., 2016. Pathological alpha-synuclein in gastrointestinal tissues from prodromal Parkinson disease patients. Ann. Neurol. 79, 940–949.
Strömberg, I., van Horne, C., Bygdeman, M., Weiner, N., Gerhardt, G.A., 1991. Function of intraventricular human mesencephalic xenografts in immunosuppressed rats: an electrophysiological and neurochemical analysis. Exp. Neurol. 112, 140–152.
Swanson, L.W., Hartman, B.K., 1975. The central adrenergic system. An immunofluorescence study of the location of cell bodies and their efferent connections in the rat utilizing dopamine-beta-hydroxylase as a marker. J. Comp. Neurol. 163, 467–505.
Szot, P., Miguelez, C., White, S.S., Franklin, A., Sikkema, C., Wilkinson, C.W., Ugedo, L., Raskind, M.A., 2010. A comprehensive analysis of the effect of DSP4 on the locus coeruleus noradrenergic system in the rat. Neuroscience 166, 279–291.
Tagliaferro, P., Burke, R.E., 2016. Retrograde Axonal degeneration in Parkinson disease. J. Parkinson's Dis. 6, 1–15.
Ungerstedt, U., 1971. Stereotaxic mapping of the monoamine pathways in the rat brain. Acta Physiol. Scand. Suppl. 367, 1–48.
van Horne, C., Hoffer, B.J., Strömberg, I., Gerhardt, G.A., 1992. Clearance and diffusion of locally applied dopamine in normal and 6-hydroxydopamine-lesioned rat striatum. J. Pharmacol. Exp. Ther. 263, 1285–1292.
Watson, M., McElligott, J.G., 1984. Cerebellar norepinephrine depletion and impaired acquisition of specific locomotor tasks in rats. Brain Res. 296, 129–138.
Wenge, B., Bonisch, H., 2009. Naunyn Schmiedebergs Arch Pharmacol. Naunyn Schmiedebergs Arch. Pharmacol 380, 523–529.
West, M.J., Slomianka, L., Gundersen, H.G.J., 1991. Unbiased stereological estimation of the total number of neurons in the subdivisions of the rat hippocampus using the optical fractionator. Anat. Rec. 231, 482–497.
Westlund, K.N., Bowker, R.M., Ziegler, M.G., Coulter, J.D., 1983. Noradrenergic projections to the spinal cord of the rat. Brain Res. 263, 15–31.
Yao, N., Wu, Y., Zhou, Y., Ju, L., Liu, Y., Ju, R., Duan, D., Xu, Q., 2015. Lesion of the locus coeruleus aggravates dopaminergic neuron degeneration by modulating microglial function in mouse models of Parkinsons disease. Brain Res. 1625, 255–274.
Zaccai, J., Brayne, C., McKeith, I., Matthews, F., Ince, P.G., Mrc Cognitive Function, A. N. S, 2008. Patterns and stages of alpha-synucleinopathy: relevance in a population-based cohort. Neurology 70, 1042–1048.
Zarow, C., Lyness, S.A., Mortimer, J.A., Chui, H.C., 2003. Neuronal loss is greater in the locus coeruleus than nucleus basalis and substantia nigra in Alzheimer and Parkinson diseases. Arch. Neurol. 60, 337–341.
Zhang, X., Zuo, D.M., Yu, P.H., 1995. Neuroprotection by R(-)-deprenyl and N-2-hexyl-N-methylpropargylamine on DSP-4, a neurotoxin, induced degeneration of noradrenergic neurons in the rat locus coeruleus. Neurosci. Lett. 186, 45–48.